Canted ferromagnetic order in nonsuperconducting Eu(Fe$_{1-x}$Ni$_x$)$_2$As$_2$

Sijie Hao,[1] Wentao Jin [ORCID],[2,*] Zbigniew Bukowski,[3] Zhengwang Lin,[2] Yinguo Xiao [ORCID],[4] and Yixi Su[5]

[1]*Department of Physics, Beijing Normal University, Beijing 100875, China*
[2]*School of Physics, Beihang University, Beijing 100191, China*
[3]*Institute of Low Temperature and Structure Research, Polish Academy of Sciences, 50-422 Wroclaw, Poland*
[4]*School of Advanced Materials, Peking University Shenzhen Graduate School, Shenzhen 518055, China*
[5]*Jülich Centre for Neutron Science JCNS at Maier-Leibnitz Zentrum (MLZ), Forschungszentrum Jülich GmbH,
Lichtenbergstraße 1, D-85747 Garching, Germany*

The magnetic order in a series of nonsuperconducting Eu(Fe$_{1-x}$Ni$_x$)$_2$As$_2$ single crystals is investigated in detail by polarized neutron diffraction. The Fe and Eu magnetic sublattices are found to be almost magnetically decoupled in this system. With the Ni doping, the Eu sublattice shows a dramatic change in its magnetic ground state, from the A-type antiferromagnetic order for $x \leqslant 0.02$, in which the spins lie in the ab plane, to a pure canted ferromagnetic order for $0.04 \leqslant x \leqslant 0.20$, in which the spins are canted with a small angle off the c axis. By comparison with the c-axis perfectly aligned ferromagnetic structure widely observed in other superconducting compounds, the lack of superconductivity in Eu(Fe$_{1-x}$Ni$_x$)$_2$As$_2$ might be associated with the formation of in-plane ferromagnetism. The doping-induced change of the lattice constants and accordingly the variation of the strength of indirect Ruderman-Kittel-Kasuya-Yosida (RKKY) interaction between the Eu^{2+} moments is speculated to be responsible for the dramatic change of the Eu spin structure. In addition, a spin reorientation of the Eu^{2+} moments in an intermediate temperature range is observed for $x = 0.20$, in which some in-plane spin fluctuations persists above the long-range ordering temperature T_{Eu}.

I. INTRODUCTION

The EuFe$_2$As$_2$-based iron pnictides have provided good opportunities to study the intriguing interplay between the magnetism and unconventional superconductivity (SC) as well as the 3d-4f interactions between the Fe and Eu magnetic sublattices [1,2]. At room temperature, EuFe$_2$As$_2$, the undoped nonsuperconducting parent compound, crystallizes in the ThCr$_2$Si$_2$ crystal structure with a tetragonal symmetry (space group $I4/mmm$). Upon cooling, it first undergoes a tetragonal-to-orthorhombic structural phase transition, accompanied by a spin-density-wave (SDW) type antiferromagnetic (AFM) ordering of the itinerant Fe-3d moments at $T_{\text{SDW}} = 190$ K. The localized Eu-4f moments order magnetically at a much lower temperature around $T_{\text{Eu}} = 19$ K in the A-type AFM structure [3–5]. The saturated moments within the Fe and Eu sublattices are determined by neutron diffraction to be ~ 1 μ_{B} and ~ 7 μ_{B}, respectively, and the moment directions are both along the longer a axis of the orthorhombic unit cell [5].

Unconventional SC can be realized in the EuFe$_2$As$_2$ system by suppressing the Fe-SDW order by means of chemical doping or applying hydrostatic pressure [1,6–11]. On the other hand, the magnetic ground state of the Eu^{2+} spins can be tuned from the A-type AFM to a purely ferromagnetic (FM) structure, as a function of doping or pressure [12–16]. For

example, an isovalent substitution of P for As leads to the emergence of bulk SC with the transition temperature between 22 and 28 K, which can microscopically coexist with the strong ferromagnetism from the Eu sublattice (with a huge moment size of ~ 7 μ_{B} per Eu atom) [7,13,17,18]. In addition, doping into the Fe sites using 3d Co, 4d Ru, or 5d Ir can also disturb the FeAs layers and result in the occurrence of SC [8,19–21]. Experimentally, it is revealed that the Eu sublattice tends to order ferromagnetically completely along its crystallographic c axis in the superconducting compositions, when the doping is above a certain level [18,22–24]. Such an intriguing doping-induced coexistence of ferromagnetism and SC in the EuFe$_2$As$_2$ system has drawn much attention in the past decade [25–29], due to potential applications in superconducting spintronics.

Unlike the case of Co doping, it was found that Ni doping into the Fe sites never leads to the SC, although it suppresses the Fe-SDW order effectively [30,31]. Therefore, the system of Eu(Fe$_{1-x}$Ni$_x$)$_2$As$_2$ provides a clean and suitable platform to probe the 3d and 4f magnetism from the Fe and Eu sublattice, respectively, without the interference of the SC. Here by means of polarized neutron diffraction on high-quality single-crystal samples, we have studied systematically the evolution of magnetic order in the Eu(Fe$_{1-x}$Ni$_x$)$_2$As$_2$ system with the Ni doping level x, and found a doping-induced dramatic change in the magnetic ground state of the Eu sublattice from the A-type AFM order to a pure canted FM order. However, the Fe and Eu magnetic sublattices are found to be almost magnetically decoupled and no evidence for a strong 3d-4f

*wtjin@buaa.edu.cn

interplay is observed in this system. The doping-induced in-plane ferromagnetism might be associated with the absence of SC in this system.

II. EXPERIMENTAL DETAILS

Single crystals of $Eu(Fe_{1-x}Ni_x)_2As_2$ with different doping levels of Ni were grown using the Sn-flux method [31]. The concentration of Ni in the obtained crystals were determined by the energy-dispersive x-ray spectroscopy (EDX) to be $x = 0.02, 0.04, 0.06,$ and 0.20. The crystals were platelike with dimensions up to $\sim 5 \times 5 \times 1$ mm^3 with the crystallographic c axis being the normal direction. The physical properties of the crystals were characterized by the resistivity and specific-heat measurements using a Quantum Design physical property measurement system (PPMS).

To probe the magnetic order microscopically, polarized neutron diffraction measurements were performed on the diffuse scattering cold-neutron spectrometer DNS at the Heinz Maier-Leibnitz Zentrum (Garching, Germany) [32], on the same crystals used in macroscopic measurements. A PG(002) monochromator was used to produce a monochromatic incident neutron beam with the wavelength of 4.2 Å. The crystals were mounted on thin aluminum plates with a tiny amount of GE varnish and put inside a standard closed-cycle cryostat, allowing them to reach a base temperature of 3.6 K. They were aligned with the [0, 1, 0] direction orienting perpendicular to the horizontal scattering plane, so that the $(H, 0, L)$ reciprocal plane can be mapped out by rotating the sample. Both the neutron polarizer and polarization analyzer at DNS are based on $m = 3$ polarizing supermirrors. A Helmholtz XYZ-coil system is used for the xyz polarization analysis. The flipping ratio of the polarized neutron setup on the studied samples is in the range of 20–25.

III. EXPERIMENTAL RESULTS

The in-plane resistivity and molar specific heat of the $Eu(Fe_{1-x}Ni_x)_2As_2$ single crystals as a function of temperature are summarized in Figs. 1(a) and 1(b), respectively. The observed high-temperature and low-temperature anomalies are associated with the Fe-SDW order [marked by vertical dashed lines in both Fig. 1(a) and Fig. 1(b)] and the magnetic order of the Eu sublattice [marked by vertical arrows in Fig. 1(b)], respectively. For comparison, the resistivity of the parent compound ($x = 0$) grown by us and the specific heat data for $x = 0$ from Ref. [33] have also been included. It is clear that the high-temperature Fe-SDW order is suppressed continuously with increasing Ni doping, from $T_{SDW} = 190$ K for $x = 0$ [3,4,33], to 164(2) K for $x = 0.02$, 104(2) K for $x = 0.04$, and finally to 65(2) K for $x = 0.06$. For $x = 0.20$, the Fe-SDW order is hardly resolved. In addition, as shown in the inset of Fig. 1(b), T_{Eu}, the ordering temperature of Eu^{2+} spins, first decreases from 19 K for $x = 0$ [3,4,33], via 17.4(1) K for $x = 0.02$, reaching a minimal value of 15.5(1) K for $x = 0.04$, and then increases upon further Ni doping, via 16.6(1) K for $x = 0.06$, finally to 19.1(1) K for $x = 0.20$. The nonmonotonic variation of T_{Eu} with x strongly suggests a possible change of the magnetic ground state of the Eu sublattice.

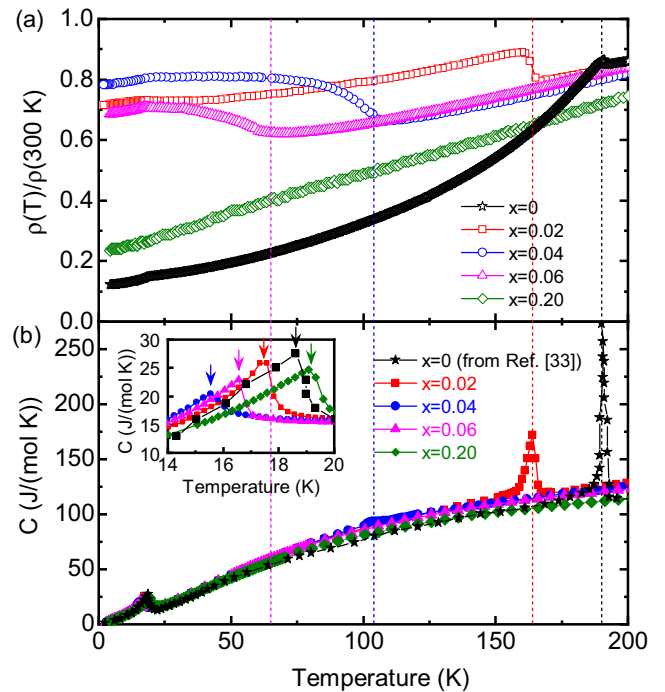FIG. 1. Temperature dependences of the normalized in-plane resistivity (a) and molar specific heat (b) of the $Eu(Fe_{1-x}Ni_x)_2As_2$ single crystals. The inset in (b) enlarges the low-temperature specific heat around T_{Eu}. The vertical dashed lines and arrows mark the Fe-SDW order and the magnetic order of Eu, respectively. The specific-heat data of the parent compound ($x = 0$) is taken from Ref. [33] for a comparison.

To probe the magnetic order in the two magnetic sublattices microscopically, polarized neutron diffraction experiments were performed on the same single-crystal samples of $Eu(Fe_{1-x}Ni_x)_2As_2$ used in the resistivity and specific-heat measurements. Figure 2 shows the temperature dependences

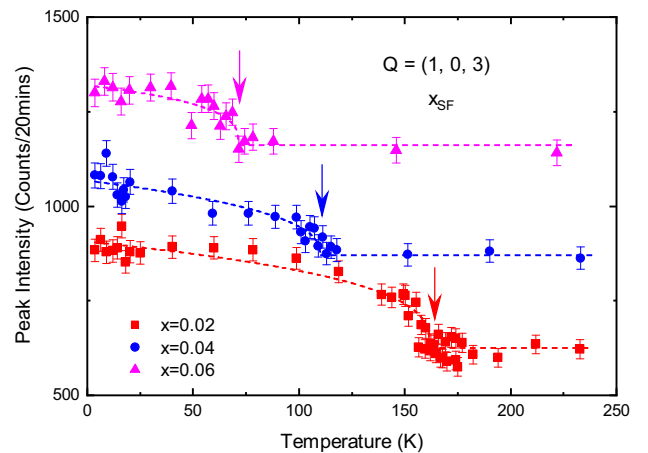FIG. 2. Temperature dependences of the peak intensities of the $(1, 0, 3)$ magnetic reflection associated with the Fe-SDW order in $Eu(Fe_{1-x}Ni_x)_2As_2$ crystals with $x = 0.02, 0.04,$ and 0.06, respectively. The vertical arrows mark T_{SDW}, the onset temperature of the Fe-SDW order. The dashed lines represent the fittings using a power law for $T < T_{SDW}$ and the background for $T > T_{SDW}$.
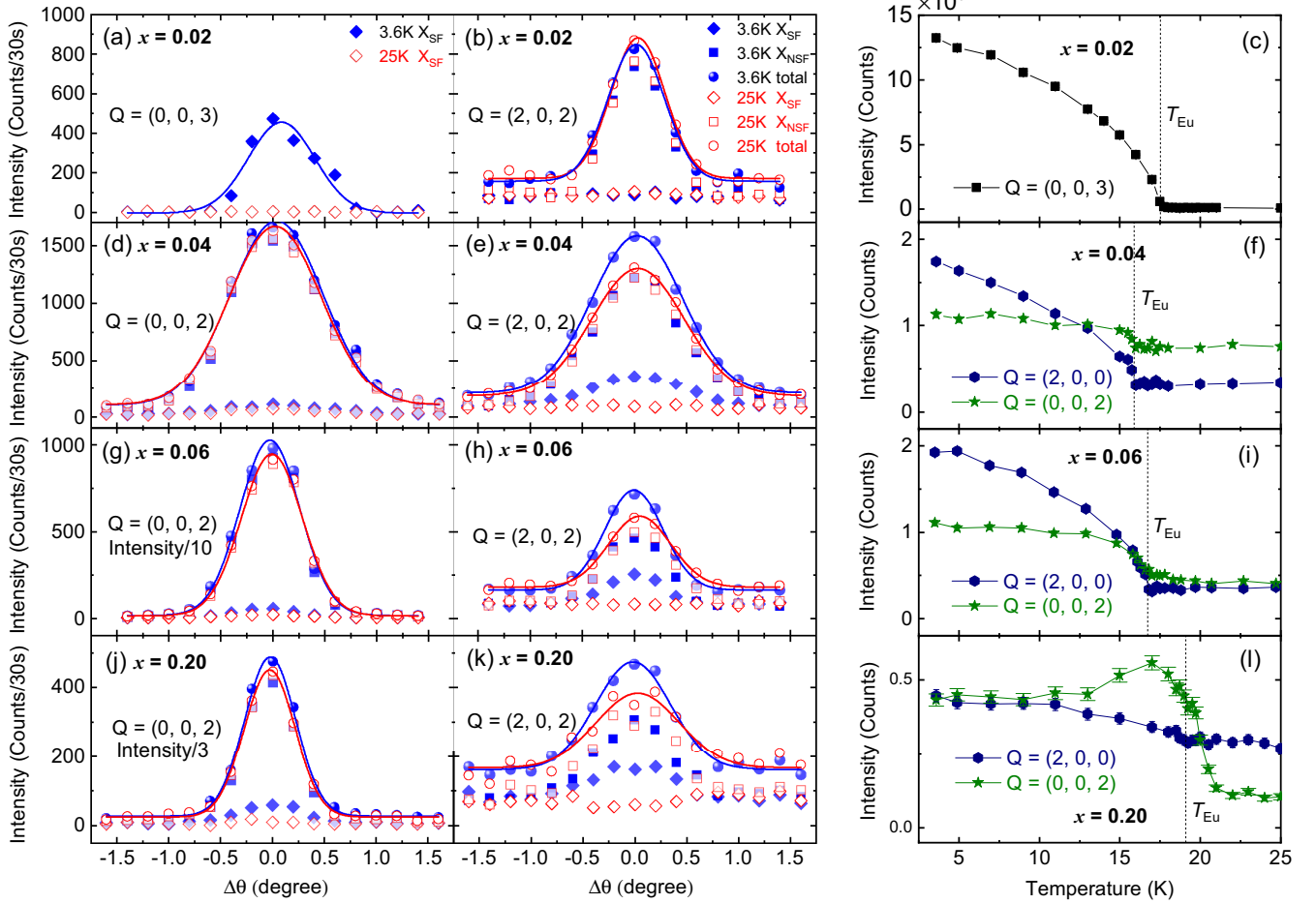
FIG. 3. Rocking-curve scans of the representative reflections in $Eu(Fe_{1-x}Ni_x)_2As_2$ crystals with $x = 0.02$ (a)–(b), 0.04 (d)–(e), 0.06 (g)–(h), and 0.20 (j)–(k), collected in the x_{SF} channel (diamonds) and x_{NSF} channel (squares), at 3.6 K (solid symbols) and 25 K (open symbols), respectively. The total intensity (circles) as the sum of those in the two channels and the fittings using a Gaussian profile (solid lines) are also shown. (c), (f), (i), and (l) show the temperature dependences of the peak intensities recorded in the x_{SF} channel for representative magnetic reflections. The counting time is 300 s for (0, 0, 3) in (c) ($x = 0.02$), 120 s for (2, 0, 0) and (0, 0, 2) in (f) ($x = 0.04$), 300 s for (2, 0, 0) and 60 s for (0, 0, 2) in (i) ($x = 0.06$), and 300 s for (2, 0, 0) and 60 s for (0, 0, 2) in (l) ($x = 0.20$). The vertical dashed lines mark T_{Eu}, the magnetic ordering temperature of Eu.

of the peak intensities of $(1, 0, 3)$ reflection for different compositions, recorded in the spin-flip channel for the x polarization (x_{SF} channel). With such a polarization, the spins of incident neutrons are polarized approximately parallel to the scattering vector Q so that the nuclear and magnetic scattering can be separated into the non-spin-flip (x_{NSF}) and spin-flip (x_{SF}) channels, respectively [34]. The scattering cross sections for the x_{NSF} and x_{SF} channels read as

$$\left(\frac{d\sigma}{d\Omega}\right)_x^{NSF} \propto N^*N + \frac{1}{3}I_{SI} \qquad (1)$$

and

$$\left(\frac{d\sigma}{d\Omega}\right)_x^{SF} \propto M_{\perp Y}^*M_{\perp Y} + M_{\perp Z}^*M_{\perp Z} + \frac{2}{3}I_{SI} \qquad (2)$$

respectively, where N^*N denotes the coherent nuclear scattering and I_{SI} denotes the spin incoherent scattering background, whereas $M_{\perp Y}^*M_{\perp Y}$ and $M_{\perp Z}^*M_{\perp Z}$ are the components of the moment parallel and perpendicular to the scattering plane,

respectively. The symbol $\perp$ indicates that the magnetic scattering is only sensitive to the component of the moment perpendicular to Q. Therefore, the appearance of the $(1, 0, 3)$ reflection in the x_{SF} channel clearly indicates its magnetic origin, as expected for the Fe-SDW order in the $EuFe_2As_2$ system with a magnetic propagation vector of $k = (1, 0, 1)$ [5]. As shown in Fig. 2, T_{SDW}, below which the intensity of the $(1, 0, 3)$ reflection increases gradually upon cooling, is suppressed by increasing Ni doping. For $x = 0.20$, no magnetic scattering was observed at $Q = (1, 0, 3)$ in the x_{SF} channel, suggesting the complete suppression of the Fe-SDW order at such a high doping level, in agreement with the absence of any anomaly in Fig. 1. The values of T_{SDW} marked by vertical arrows in Fig. 2 are very consistent with those determined by macroscopic measurements shown in Fig. 1.

The magnetic ground state of the Eu sublattice as a function of Ni doping level is also determined by polarized neutron diffraction. As shown in Fig. 3(a), for $x = 0.02$, a forbidden Bragg reflection $(0, 0, 3)$ with the magnetic propagation vector $k = (0, 0, 1)$, is observed in the x_{SF} (magnetic scattering)

channel at 3.6 K and disappears at 25 K well above T_{Eu}. In addition, for a nuclear reflection $(2, 0, 2)$, no intensities are observed at 3.6 K in the x_{SF} channel [see Fig. 3(b)]. Almost the same intensities are recorded for $(2, 0, 2)$ at 3.6 and 25 K in the x_{NSF} channel (nuclear plus spin incoherent scattering), together with the unchanged intensities of the total scattering (sum of the x_{SF} and x_{NSF} channels), suggesting that there are no ferromagnetic contributions arising from a possible out-of-plane canting of the Eu^{2+} spins, which will lead to magnetic scatterings in the x_{SF} channel and a decrease of intensities in the x_{NSF} channel due to the neutron-depolarization effect for $T < T_{Eu}$ [14]. Therefore, the magnetic order of the Eu sublattice for $x = 0.02$ is a pure A-type AFM structure without any spin canting, the same as the undoped parent compound [5].

The situation changes with further Ni doping, as the $(0, 0, odd)$ reflections are no longer observed for the other three compositions ($x = 0.04$, 0.06, and 0.20). In contrast, in the x_{SF} channel, additional intensities show up below T_{Eu} for the nuclear reflections $(2, 0, 0)$, $(0, 0, 2)$, and $(2, 0, 2)$, indicating a magnetic propagation vector $k = 0$ and the formation of a pure ferromagnetically ordered Eu sublattice starting from $x = 0.04$. Figures 3(d)–3(e), 3(g)–3(h), and 3(j)–3(k) show the rocking-curve scans of the $(0, 0, 2)$ and $(2, 0, 2)$ reflections recorded in the x_{SF} and x_{NSF} channels for the three compositions, as well as the total intensities as the sum of the two channels, at the base temperature and 25 K (well above T_{Eu}) for comparison. Considering the neutron-depolarization effect caused by the ferromagnetism and the possible imperfect separation of magnetic and nuclear scatterings into the two channels, the comparison of the total intensities of $(0, 0, 2)$ and $(2, 0, 2)$ at the two temperatures, instead of the x_{SF}-channel intensities only, can provide a more reliable basis for estimating the direction of the Eu^{2+} spins.

Different from the cases in the Co-doped $EuFe_2As_2$ system [14], in which the Eu^{2+} moments order completely along the c axis in the FM state, here the Eu^{2+} spins in $Eu(Fe_{1-x}Ni_x)_2As_2$ are believed to display a canted FM structure with their direction deviating slightly from the c axis, for $x = 0.04$, 0.06, and 0.20. This conclusion is evidenced from the clear increase of the intensities of the $(0, 0, 2)$ reflection below T_{Eu}, in both the x_{SF} channel and the total scattering, as shown in Figs. 3(d), 3(g) and 3(j). As $k = 0$ allows the Eu^{2+} moments to have ferromagnetic components both along the c axis and the ab plane, the low-$Q(0, 0, 2)$ reflection with a large magnetic form factor provides a relatively sensitive probe to the in-plane component of the FM Eu^{2+} moments, as the magnetic neutron scattering at a certain scattering vector Q arises from the magnetic moments perpendicular to Q.

The total intensity of the x_{SF} and x_{NSF} channels at 25 K is taken as the background from the nuclear plus spin incoherent scattering, since it is well above T_{Eu} and there is no magnetic scattering in the paramagnetic state, and the difference between the total intensities at 3.6 and 25 K is taken as the magnetic scattering. The rocking-curve scans of the $(0, 0, 2)$ peak shown in Figs. 3(d), 3(g) and 3(j) are fitted using a Gaussian profile, and the intensities of the magnetic (I_M) and the nuclear plus spin incoherent scattering ($I_N + I_{SI}$) are estimated and listed in Table I. Assuming that the Eu^{2+} spins own a full saturated moment of 7 μ_B at 3.6 K as expected for $S = 7/2$, the ground-state canting angle (θ) of the Eu^{2+} moments off

TABLE I. The intensities of the magnetic scattering (I_M) and the nuclear plus spin incoherent scattering ($I_N + I_{SI}$) for the $(0, 0, 2)$ reflection extracted from the fittings to the rocking curves, with $I_N + I_{SI} = x_{SF}(25\,\text{K}) + x_{NSF}(25\,\text{K})$ and $I_M = x_{SF}(3.6\,\text{K}) + x_{NSF}(3.6\,\text{K}) - x_{SF}(25\,\text{K}) - x_{NSF}(25\,\text{K})$, the ratio R between them, and the estimated canting angle (θ) of the Eu^{2+} moments off the c axis in the FM compositions. Note that the absolute numbers of I_M and $I_N + I_{SI}$ depend largely on the sample size and shape, but the ratio R is independent of these factors.

	I_M	$I_N + I_{SI}$	$R = \frac{I_M}{I_N + I_{SI}}$	Canting angle θ (deg)
$x = 0.04$	55(8)	1749(4)	0.031±0.005	7.7±0.6
$x = 0.06$	476(20)	6865(9)	0.069±0.003	11.5±0.3
$x = 0.20$	71(13)	786(7)	0.090±0.017	13.2±1.2

the c axis, which is their only degree of freedom, can be calculated based on the intensity ratio (R) between I_M and $I_N + I_{SI}$. It is found that the value of θ increases monotonically with increasing Ni doping, from $\sim 8°$ for $x = 0.04$ to $\sim 13°$ for $x = 0.20$.

In addition, the order parameter associated with the static magnetism of Eu is also measured using the scattering intensities in the x_{SF} channel for all compositions. As shown in Fig. 3(c), the temperature dependence of the peak intensity of the $(0, 0, 3)$ reflection for $x = 0.02$ indicates a second-order AFM transition below $T_{Eu} = 17.6(1)$ K. Upon further Ni doping, the A-type AFM of Eu is suppressed and a pure FM order is established starting from $x = 0.04$ already. The intensities of the $(2, 0, 0)$ and $(0, 0, 2)$ reflections, which are sensitive to the c-axis and in-plane FM Eu^{2+} moments, respectively, exhibit the same onset temperatures of $T_{Eu} = 15.9(2)$ K and $16.8(2)$ K, for $x = 0.04$ and 0.06, respectively [see Figs. 3(f) and 3(i)]. The T_{Eu} values determined here using neutrons agree well with those determined by specific-heat measurements represented above. However, it is worth noting that, for the composition with a high Ni doping level of $x = 0.20$, the intensity of the $(0, 0, 2)$ reflection shows a very distinct behavior with the temperature. As shown in Fig. 3(l), the $(2, 0, 0)$ reflection features an onset temperature of the c-axis FM moments at 19.1(2) K, very consistent with $T_{Eu} = 19.1(1)$ K determined from the heat capacity data. In contrast, the $(0, 0, 2)$ peak intensity shows a nonmonotonic variation, revealing a temperature-induced spin reorientation behavior of the Eu^{2+} moments for $x = 0.20$. Note that the intensities of both $(0, 0, 2)$ and $(2, 0, 0)$ are almost constant for $T < 10$ K, while they show opposite tendencies in the intermediate range for $10 < T < 17$ K. Starting from a canted FM structure as shown in Fig. 4(d), the rise of $(0, 0, 2)$ intensity with increasing temperature suggests the further rotation of the Eu^{2+} spins towards the ab plane, competing with the vanishing moment size upon warming. Furthermore, the disappearance of the magnetic intensity at $(0, 0, 2)$ occurs at a higher temperature of 21(1) K, compared with that of $(2, 0, 0)$ at 19.1(1) K, indicating the remnant of some in-plane spin fluctuations near the critical region above T_{Eu}.

IV. DISCUSSION AND CONCLUSION

The magnetic structure in the $Eu(Fe_{1-x}Ni_x)_2As_2$ system as a function of the Ni content x is illustrated in Fig. 4,

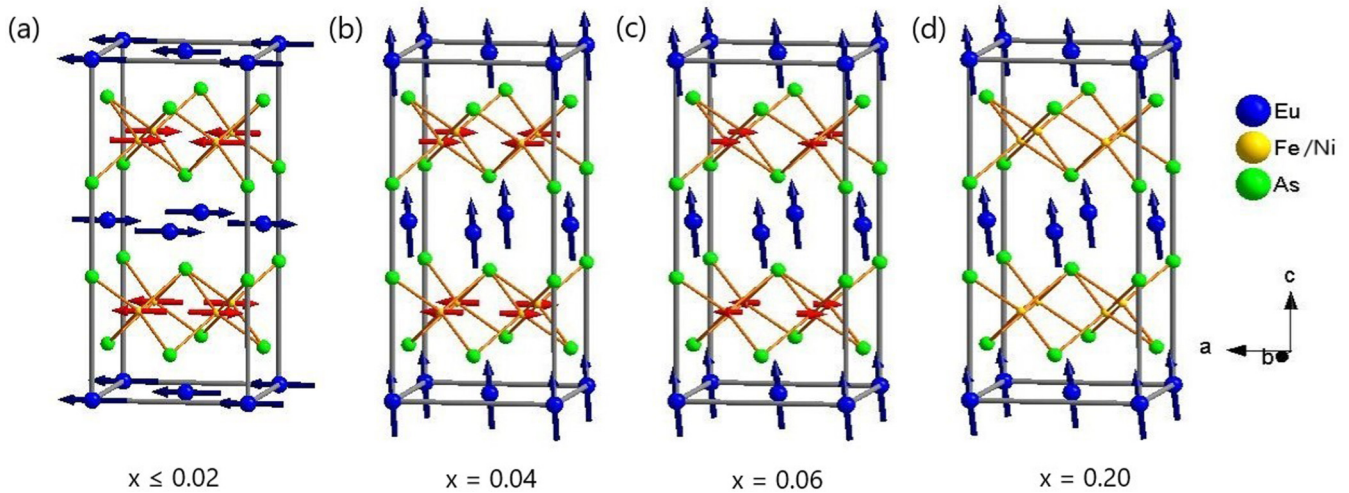FIG. 4. The ground-state ($T = 3.6$ K) magnetic structure of Eu(Fe$_{1-x}$Ni$_x$)$_2$As$_2$ for $x \leqslant 0.02$ (a), $x = 0.04$ (b), $x = 0.06$ (c), and $x = 0.20$ (d), as determined by polarized neutron diffraction. The Eu^{2+} spins in (b)–(d) are canted off the c axis with angles of 7.7($\pm$0.6)°, 11.5($\pm$0.3)°, and 13.2($\pm$1.2)°, respectively.

corresponding to a magnetic space group of $P_c bca$ (No. 61.439) for (a), $P2'/m'$ (No. 10.46) for (b) and (c), $C2'/m'$ (12.62) for (d). As no evidence for a spin reorientation of the Fe^{2+} moments (such as a sudden rise or drop of the magnetic intensity superimposed on the smooth magnetic order parameter [35,36]) is observed in Fig. 2 for $x = 0.02$, 0.04, and 0.06, it is believed that the Fe^{2+} moments keep lying in the ab plane for this system. The lack of a response near T_{Eu} in the temperature dependences of the $(1, 0, 3)$ magnetic reflection due to the Fe-SDW order suggests that the Fe and Eu sublattices are almost magnetically decoupled in Eu(Fe$_{1-x}$Ni$_x$)$_2$As$_2$.

On the other hand, the magnetic ground state of the Eu sublattice shows a dramatic change from the A-type AFM structure with $k = (0, 0, 1)$ for $x = 0.02$, the same as the parent compound, to a canted FM structure with $k = 0$ for $x \geqslant 0.04$. The Eu^{2+} moments completely lie in the ab plane for the former, but are almost aligned along the c axis for the latter with a small deviation angle (θ) slightly enlarged with increasing Ni doping. This evolution of the Eu magnetic ordering from AFM to FM was previously proposed to be induced by Ni doping above a critical doping level of 2.5%, according to a magnetic susceptibility measurement on polycrystalline samples of Eu(Fe$_{1-x}$Ni$_x$)$_2$As$_2$ [30], which is perfectly consistent with our results obtained by polarized neutron diffraction.

For $x = 0.02$ with the A-type AFM structure of Eu, as shown in Fig. 4(a), the absence of Eu-Fe coupling is not surprising, since the net field acting on the Fe site from the Eu layers is zero and no significant magnetic coupling is expected. However, for $x \geqslant 0.04$ with the canted FM structure of Eu, as shown in Figs. 4(b)–4(d), the situation is different because the Eu layers is supposed to generate a small net in-plane field at the Fe site. Therefore, the seemingly decoupled Eu-Fe magnetism for $x = 0.04$ and $x = 0.06$ in Fig. 2 is most likely due to the weakness of the effective field acting on the Fe site associated with the small canting angle of the Eu^{2+} moments.

Combining all results from the macroscopic measurements and the polarized neutron diffraction experiments presented above, a phase diagram describing the evolution of magnetic order with the Ni content in Eu(Fe$_{1-x}$Ni$_x$)$_2$As$_2$ system is established, as shown in Fig. 5. Similarly to other iron pnictides, doping suppresses the Fe-SDW order effectively, although no SC is realized in this system. However, the sharp transition in the Eu sublattice from the A-type AFM order ($x \leqslant 0.02$) to the canted FM order ($x \geqslant 0.04$), as well as the dramatic change of the moment direction, within a very narrow regime is quite unusual. This is in stark contrast to the case in Eu(Fe$_{1-x}$Co$_x$)$_2$As$_2$, in which the crossover from the A-type AFM structure to the pure FM structure is

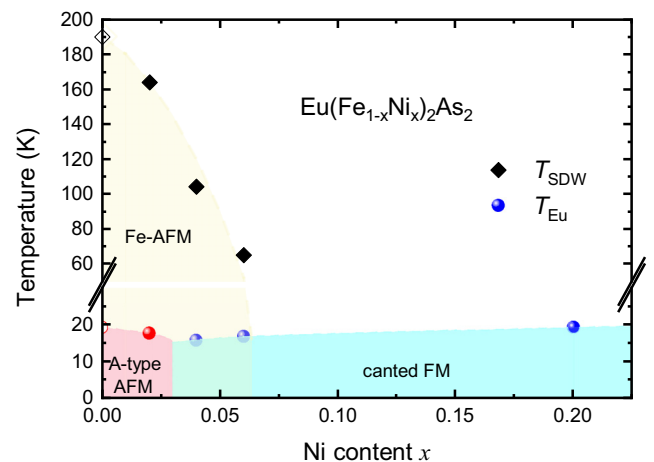FIG. 5. The phase diagram of the Eu(Fe$_{1-x}$Ni$_x$)$_2$As$_2$ system for $x \leqslant 0.20$, illustrating the evolution of the magnetic order with Ni doping. The T_{SDW} and T_{Eu} values for the parent compound ($x = 0$) are obtained from Ref. [5]. The yellow, red, and blue regions represent the Fe-AFM state, A-type AFM state of Eu, and canted FM state of Eu, respectively.

realized by passing a broad intermediate canted AFM state with two k vectors of $(0, 0, 1)$ and $(0, 0, 0)$ simultaneously [14]. Since the Eu layers are well separated and the $4f$ Eu^{2+} moments are quite localized, the direct exchange interactions can be neglected. Therefore, the interlayer coupling responsible for the three-dimensional (3D) magnetic ordering of the Eu sublattice is speculated to arise from the indirect Ruderman-Kittel-Kasuya-Yosida (RKKY) interaction mediated by the conduction d electrons on the FeAs layers [37–40], which is discussed in details in Ref. [30]. To be concise, the RKKY coupling takes the form of $J_{RKKY} \propto -\frac{\alpha \cos\alpha - \sin\alpha}{\alpha^4}$, where $\alpha = 2k_F R$ (k_F is the Fermi vector and R is the distance between two magnetic moments). Since the 3D hole pocket of the Fermi surface derived from the d electrons of Fe is most likely to be responsible for mediating the RKKY interaction, the substitution of Ni^{2+} ($3d^8$) for Fe^{2+} ($3d^6$) will lead to electron doping and an effective shrinkage of k_F. In the meantime, R also decreases due to the contraction of the lattice constant c with Ni doping [30,31]. As a result, it is expected that the sign of J_{RKKY} will oscillate between negative and positive, with the variation of $k_F R$ as a function of the Ni doping level x. Accordingly, the interlayer coupling between the Eu layers can be tuned from AFM to FM above certain x. Here in $Eu(Fe_{1-x}Ni_x)_2As_2$, the rapid change of the magnetic ground state for $0.02 \leqslant x \leqslant 0.04$ might result from a more drastic reduction of the lattice constants c (and accordingly $k_F R$) in this doping range, as reported in a recent experimental study on the $Eu(Fe_{1-x}Ni_x)_2As_2$ crystals grown from the same batch as those used in our study [31], which may cause a sign change of J_{RKKY}. Further experimental and theoretical studies will be valuable to verify such a scenario.

We note that such a canted FM structure observed here in $Eu(Fe_{1-x}Ni_x)_2As_2$ for $x \geqslant 0.04$ was previously experimentally observed for nonsuperconducting $EuFe_2P_2$ using Mössbauer and neutron diffraction measurements [41,42], which was ascribed to the combined effect of indirect RKKY interaction and direct Fe-Eu exchange interaction. On the other hand, in the doped $EuFe_2As_2$ compounds that are superconducting, it has been widely experimentally revealed that the Eu^{2+} moments are perfectly aligned along the c axis and there is no in-plane FM order due to the spin canting [18,22–24]. The absence of SC in $Eu(Fe_{1-x}Ni_x)_2As_2$ was discussed in Ref. [30] and ascribed to the adverse effect of RKKY interaction responsible for the Eu magnetic ordering, which is established prior to the possible superconducting transition upon cooling and hinders the Cooper pairing. Here we propose an alternative scenario that the formation of in-plane FM order of the Eu^{2+} moments, in the canted FM structure, might be incompatible with the SC by acting an in-plane polarizing field and destroying the superconducting Cooper pairs more effectively.

It is worth noting that the Ni-doping-induced modification of the ground-state magnetic structure of the Eu sublattice

was also reported recently in $RbEu(Fe_{1-x}Ni_x)_4As_4$, a novel family of the Fe-based superconductors, evolving smoothly from a helical order to a collinear FM order with x [43]. The variation of the rotation angle between adjacent Eu^{2+} layers there can be well explained by considering the change of magnetic exchange couplings mediated by the indirect RKKY interaction, and the collinear FM structure with a strong in-plane FM order is only observed in the nonsuperconducting composition of $RbEu(Fe_{1-x}Ni_x)_4As_4$, somehow suggesting the incompatibility of the in-plane ferromagnetism of Eu and the SC as discussed above for $Eu(Fe_{1-x}Ni_x)_2As_2$.

It is also found by neutron diffraction that, in the end member $EuNi_2As_2$ ($x = 1$), the Eu^{2+} moments lie completely in the ab plane and form a helical order with an incommensurate magnetic propagation vector $k = (0, 0, 0.92)$ [44]. Therefore, it is expected that another transition from the canted FM order to the helical order will occur at a higher Ni doping level in between 0.20 and 1, awaiting further experimental verifications once high-quality single-crystal samples are available.

In conclusion, the magnetic orders in nonsuperconducting $Eu(Fe_{1-x}Ni_x)_2As_2$ single crystals are investigated systematically using polarized neutron diffraction. The Fe-SDW order is suppressed effectively by the Ni doping and cannot be resolved for $x = 0.20$. The magnetic ground state of the Eu sublattice shows a dramatic change from the A-type AFM order for $x \leqslant 0.02$, in which the Eu^{2+} moments lie in the ab plane, to a pure FM order for $0.04 \leqslant x \leqslant 0.20$, in which the Eu^{2+} moments are canted with a small angle off the c axis. Such a doping-induced transition is speculated to arise from the change of lattice constants and accordingly the variation of the strength of indirect RKKY interaction between the Eu^{2+} moments. The lack of SC in this system might be associated with the formation of in-plane ferromagnetism. A spin reorientation of the Eu^{2+} moments is observed in the intermediate range for $10 < T < 17$ K for $x = 0.20$, in which in-plane spin fluctuations persists above the long-range ordering temperature T_{Eu}. No evidence for a strong interplay between the $3d$ and $4f$ magnetism from the Fe and Eu sublattice, respectively, is observed in this system.

[1] S. Zapf and M. Dressel, Europium-based iron pnictides: A unique laboratory for magnetism, superconductivity and structural effects, Rep. Prog. Phys. **80**, 016501 (2017).

[2] J. Maiwald and P. Gegenwart, Interplay of 4f and 3d moments in $EuFe_2As_2$ iron pnictides, Phys. Status Solidi B **254**, 1600150 (2017).

[3] H. S. Jeevan, Z. Hossain, D. Kasinathan, H. Rosner, C. Geibel, and P. Gegenwart, Electrical resistivity and specific heat of single-crystalline EuFe$_2$As$_2$: A magnetic homologue of SrFe$_2$As$_2$, Phys. Rev. B **78**, 052502 (2008).

[4] Z. Ren, Z. Zhu, S. Jiang, X. Xu, Q. Tao, C. Wang, C. Feng, G. Cao, and Z. Xu, Antiferromagnetic transition in EuFe$_2$As$_2$: A possible parent compound for superconductors, Phys. Rev. B **78**, 052501 (2008).

[5] Y. Xiao, Y. Su, M. Meven, R. Mittal, C. M. N. Kumar, T. Chatterji, S. Price, J. Persson, N. Kumar, S. K. Dhar, A. Thamizhavel, and T. Brueckel, Magnetic structure of EuFe$_2$As$_2$ determined by single-crystal neutron diffraction, Phys. Rev. B **80**, 174424 (2009).

[6] H. S. Jeevan, Z. Hossain, D. Kasinathan, H. Rosner, C. Geibel, and P. Gegenwart, High-temperature superconductivity in Eu$_{0.5}$K$_{0.5}$Fe$_2$As$_2$, Phys. Rev. B **78**, 092406 (2008).

[7] Z. Ren, Q. Tao, S. Jiang, C. Feng, C. Wang, J. Dai, G. Cao, and Z. Xu, Superconductivity Induced by Phosphorus Doping and Its Coexistence with Ferromagnetism in EuFe$_2$(As$_{0.7}$P$_{0.3}$)$_2$, Phys. Rev. Lett. **102**, 137002 (2009).

[8] W. H. Jiao, Q. Tao, J. K. Bao, Y. L. Sun, C. M. Feng, Z. A. Xu, I. Nowik, I. Felner, and G. H. Cao, Anisotropic superconductivity in Eu(Fe$_{0.75}$Ru$_{0.25}$)$_2$As$_2$ ferromagnetic superconductor, Europhys. Lett. **95**, 67007 (2011).

[9] C. F. Miclea, M. Nicklas, H. S. Jeevan, D. Kasinathan, Z. Hossain, H. Rosner, P. Gegenwart, C. Geibel, and F. Steglich, Evidence for a reentrant superconducting state in EuFe$_2$As$_2$ under pressure, Phys. Rev. B **79**, 212509 (2009).

[10] T. Terashima, M. Kimata, H. Satsukawa, A. Harada, K. Hazama, S. Uji, H. S. Suzuki, T. Matsumoto, and K. Murata, EuFe$_2$As$_2$ under high pressure: An antiferromagnetic bulk superconductor, J. Phys. Soc. Jpn. **78**, 083701 (2009).

[11] W. T. Jin, Y. Xiao, S. Nandi, S. Price, Y. Su, K. Schmalzl, W. Schmidt, T. Chatterji, A. Thamizhavel, and T. Brückel, Coexistence of Eu antiferromagnetism and pressure-induced superconductivity in single-crystal EuFe$_2$As$_2$, Phys. Rev. B **100**, 014503 (2019).

[12] H. S. Jeevan, D. Kasinathan, H. Rosner, and P. Gegenwart, Interplay of antiferromagnetism, ferromagnetism, and superconductivity in EuFe$_2$(As$_{1-x}$P$_x$)$_2$ single crystals, Phys. Rev. B **83**, 054511 (2011).

[13] G. H. Cao, S. G. Xu, Z. Ren, S. Jiang, C. M. Feng, and Z. A. Xu, Superconductivity and ferromagnetism in EuFe$_2$(As$_{1-x}$P$_x$)$_2$, J. Phys.: Condens. Matter **23**, 464204 (2011).

[14] W. T. Jin, Y. Xiao, Z. Bukowski, Y. Su, S. Nandi, A. P. Sazonov, M. Meven, O. Zaharko, S. Demirdis, K. Nemkovski, K. Schmalzl, L. M. Tran, Z. Guguchia, E. Feng, Z. Fu, and T. Brückel, Phase diagram of Eu magnetic ordering in Sn-flux-grown Eu(Fe$_{1-x}$Co$_x$)$_2$As$_2$ single crystals, Phys. Rev. B **94**, 184513 (2016).

[15] K. Matsubayashi, K. Munakata, M. Isobe, N. Katayama, K. Ohgushi, Y. Ueda, N. Kawamura, M. Mizumaki, N. Ishimatsu, M. Hedo, I. Umehara, and Y. Uwatoko, Pressure-induced changes in the magnetic and valence state of EuFe$_2$As$_2$, Phys. Rev. B **84**, 024502 (2011).

[16] Z. Guguchia, A. Shengelaya, A. Maisuradze, L. Howard, Z. Bukowski, M. Chikovani, H. Luetkens, S. Katrych, J. Karpinski, and H. Keller, Muon-spin rotation and magnetization studies of chemical and hydrostatic pressure effects in EuFe$_2$(As$_{1-x}$P$_x$)$_2$, J. Supercond. Nov. Magn. **26**, 285 (2013).

[17] S. Nandi, W. T. Jin, Y. Xiao, Y. Su, S. Price, D. K. Shukla, J. Strempfer, H. S. Jeevan, P. Gegenwart, and T. Brückel, Coexistence of superconductivity and ferromagnetism in P-doped EuFe$_2$As$_2$, Phys. Rev. B **89**, 014512 (2014).

[18] S. Nandi, W. T. Jin, Y. Xiao, Y. Su, S. Price, W. Schmidt, K. Schmalzl, T. Chatterji, H. S. Jeevan, P. Gegenwart, and T. Brückel, Magnetic structure of the Eu^{2+} moments in superconducting EuFe$_2$(As$_{1-x}$P$_x$)$_2$ with $x = 0.19$, Phys. Rev. B **90**, 094407 (2014).

[19] S. Jiang, H. Xing, G. Xuan, Z. Ren, C. Wang, Z.-A. Xu, and G. Cao, Superconductivity and local-moment magnetism in Eu(Fe$_{0.89}$Co$_{0.11}$)$_2$As$_2$, Phys. Rev. B **80**, 184514 (2009).

[20] A. Błachowski, K. Ruebenbauer, J. Zukrowski, Z. Bukowski, K. Rogacki, P. J. W. Moll, and J. Karpinski, Interplay between magnetism and superconductivity in EuFe$_{2-x}$Co$_x$As$_2$ studied by ^{57}Fe and ^{151}Eu Mössbauer spectroscopy, Phys. Rev. B **84**, 174503 (2011).

[21] W. H. Jiao, H. F. Zhai, J. K. Bao, Y. K. Luo, Q. Tao, C. M. Feng, Z. A. Xu, and G. H. Cao, Anomalous critical fields and the absence of Meissner state in Eu(Fe$_{0.88}$Ir$_{0.12}$)$_2$As$_2$ crystals, New J. Phys. **15**, 113002 (2013).

[22] W. T. Jin, S. Nandi, Y. Xiao, Y. Su, O. Zaharko, Z. Guguchia, Z. Bukowski, S. Price, W. H. Jiao, G. H. Cao, and T. Brückel, Magnetic structure of superconducting Eu(Fe$_{0.82}$Co$_{0.18}$)$_2$As$_2$ as revealed by single-crystal neutron diffraction, Phys. Rev. B **88**, 214516 (2013).

[23] W. T. Jin, W. Li, Y. Su, S. Nandi, Y. Xiao, W. H. Jiao, M. Meven, A. P. Sazonov, E. Feng, Y. Chen, C. S. Ting, G. H. Cao, and T. Brückel, Magnetic ground state of superconducting Eu(Fe$_{0.88}$Ir$_{0.12}$)$_2$As$_2$: A combined neutron diffraction and first-principles calculation study, Phys. Rev. B **91**, 064506 (2015).

[24] Z. Zhou, W. T. Jin, W. Li, S. Nandi, B. Ouladdiaf, Z. Yan, X. Wei, X. Xu, W. H. Jiao, N. Qureshi, Y. Xiao, Y. Su, G. H. Cao, and T. Brückel, Universal critical behavior in the ferromagnetic superconductor Eu(Fe$_{0.75}$Ru$_{0.25}$)$_2$As$_2$, Phys. Rev. B **100**, 060406(R) (2019).

[25] W.-H. Jiao, Q. Tao, Z. Ren, Y. Liu, and G.-H. Cao, Evidence of spontaneous vortex ground state in an iron-based ferromagnetic superconductor, npj Quantum Mater. **2**, 50 (2017).

[26] V. S. Stolyarov, I. S. Veshchunov, S. Y. Grebenchuk, D. S. Baranov, I. A. Golovchanskiy, A. G. Shishkin, N. Zhou, Z. Shi, X. Xu, S. Pyon, Y. Sun, W. Jiao, G.-H. Cao, L. Y. Vinnikov, A. A. Golubov, T. Tamegai, A. I. Buzdin, and D. Roditchev, Domain Meissner state and spontaneous vortex-antivortex generation in the ferromagnetic superconductor EuFe$_2$(As$_{0.79}$P$_{0.21}$)$_2$, Sci. Adv. **4**, eaat1061 (2018).

[27] Z. Devizorova, S. Mironov, and A. Buzdin, Theory of Magnetic Domain Phases in Ferromagnetic Superconductors, Phys. Rev. Lett. **122**, 117002 (2019).

[28] G. Prando, D. Torsello, S. Sanna, M. J. Graf, S. Pyon, T. Tamegai, P. Carretta, and G. Ghigo, Complex vortex-antivortex dynamics in the magnetic superconductor EuFe$_2$(As$_{0.7}$P$_{0.3}$)$_2$, Phys. Rev. B **105**, 224504 (2022).

[29] W. Jin, S. Mühlbauer, P. Bender, Y. Liu, S. Demirdis, Z. Fu, Y. Xiao, S. Nandi, G.-H. Cao, Y. Su, and T. Brückel, Bulk domain Meissner state in the ferromagnetic superconductor EuFe$_2$(As$_{0.8}$P$_{0.2}$): Consequence of compromise between ferromagnetism and superconductivity, Phys. Rev. B **105**, L180504 (2022).

[30] Z. Ren, X. Lin, Q. Tao, S. Jiang, Z. Zhu, C. Wang, G. Cao, and Z. Xu, Suppression of spin-density-wave transition and emergence of ferromagnetic ordering of Eu^{2+} moments in $EuFe_{2-x}Ni_xAs_2$, Phys. Rev. B **79**, 094426 (2009).

[31] K. Komȩdera, J. Gatlik, B. Błachowski, J. Żukrowski, D. Rybicki, A. Delekta, M. Babij, and Z. Bukowski, ^{57}Fe and ^{151}Eu Mössbauer studies of $3d$-$4f$ spin interplay in $EuFe_{2-x}Ni_xAs_2$, Sci. Rep. **11**, 11484 (2021).

[32] Y. Su, K. Nemkovskiy, and S. Demirdis, DNS: Diffuse scattering neutron time-of-flight spectrometer, J. Large-Scale Res. Facil. **1**, A27 (2015).

[33] J. Herrero-Martín, V. Scagnoli, C. Mazzoli, Y. Su, R. Mittal, Y. Xiao, T. Brueckel, N. Kumar, S. K. Dhar, A. Thamizhavel, and L. Paolasini, Magnetic structure of $EuFe_2As_2$ as determined by resonant x-ray scattering, Phys. Rev. B **80**, 134411 (2009).

[34] O. Schärpf and H. Capellmann, The XYZ-difference method with polarized neutrons and the separation of coherent, spin incoherent, and magnetic scattering cross sections in a multi-detector, Phys. Stat. Sol. A **135**, 359 (1993).

[35] W. T. Jin, M. Meven, A. P. Sazonov, S. Demirdis, Y. Su, Y. Xiao, Z. Bukowski, S. Nandi, and T. Brückel, Spin reorientation of the Fe moments in $Eu_{0.5}Ca_{0.5}Fe_2As_2$: Evidence for strong interplay of Eu and Fe magnetism, Phys. Rev. B **99**, 140402(R) (2019).

[36] F. Waßer, A. Schneidewind, Y. Sidis, S. Wurmehl, S. Aswartham, B. Büchner, and M. Braden, Spin reorientation in $Ba_{0.65}Na_{0.35}Fe_2As_2$ studied by single-crystal neutron diffraction, Phys. Rev. B **91**, 060505(R) (2015).

[37] M. A. Ruderman and C. Kittel, Indirect exchange coupling of nuclear magnetic moments by conduction electrons, Phys. Rev. **96**, 99 (1954).

[38] T. Kasuya, A theory of metallic ferro- and antiferromagnetism on Zener's model, Prog. Theor. Phys. **16**, 45 (1956).

[39] K. Yosida, Magnetic properties of Cu-Mn alloys, Phys. Rev. **106**, 893 (1957).

[40] A. Akbari, P. Thalmeier, and I. Eremin, Evolution of the multiband Ruderman-Kittel-Kasuya-Yoshida interaction: Application to iron pnictides and chalcogenides, New J. Phys. **15**, 033034 (2013).

[41] C. Feng, Z. Ren, S. Xu, S. Jiang, Z. Xu, G. Cao, I. Nowik, I. Felner, K. Matsubayashi, and Y. Uwatoko, Magnetic ordering and dense Kondo behavior in $EuFe_2P_2$, Phys. Rev. B **82**, 094426 (2010).

[42] D. H. Ryan, J. M. Cadogan, S. Xu, Z. Xu, and G. Cao, Magnetic structure of $EuFe_2P_2$ studied by neutron powder diffraction, Phys. Rev. B **83**, 132403 (2011).

[43] Q. Xu, Y. Liu, S. Hao, J. Qian, C. Su, C.-W. Wang, T. Hansen, Z. Fu, Y. Su, W. Li, G.-H. Cao, Y. Xiao, and W. Jin, Evolution from helical to collinear ferromagnetic order of the Eu^{2+} spins in $RbEu(Fe_{1-x}Ni_x)_4As_4$, Phys. Rev. Res. **4**, 013077 (2022).

[44] W. T. Jin, N. Qureshi, Z. Bukowski, Y. Xiao, S. Nandi, M. Babij, Z. Fu, Y. Su, and T. Brückel, Spiral magnetic ordering of the Eu moments in $EuNi_2As_2$, Phys. Rev. B **99**, 014425 (2019).